[논 문] 한국재료학회지
Korean Journal of Materials Research
Vol. 5, No. 7 (1995)

Hadfield강에서의 마르텐사이트 상변태와 결정방위조직과의 관계 연구

김 택 남
배재대학교 무기재료공학과

The Martensitic Phase Transformation and Texture Development in Hadfield's Steels

Taik Nam Kim
Department of Inorganic Materials Engineering, Pai Chai University, Taejon, Korea

요 약 다른 탄소함량을 갖는 두 Hadfield 강에서 압연에 따른 결정방위조직(Texture)과 마르텐사이트 상변태를 연구하였다(0.65wt.%, 1.35wt.%) 두 Hadfield 강의 적층결함에너지 차이가 매우 적음에도 불구하고 (약 2mJm^{-2}) 결정방위조직은 차이를 보였다. 0.65wt.% 탄소 강의 경우, 낮은 변형구간에서는 낮은 적층에너지 금속과 비슷한 결정방위조직을 보였으나 높은 변형에서는 {111}<uvw>, {110}<001>과 같은 이상 결정방위조직이 나타났고, 이것은 입계 또는 일단의 전단띠에(shear bands) 형성된 α 마르텐사이트의 방해에 의한 것으로 생각된다. 이와는 대조적으로 1.35wt.% Hadfield강은 전변형구간에서 낮은 적층결함에너지를 갖는 금속과 비슷한 결정방위조직을 보이고 있다. 이것은 변형중에 유도된 마르텐사이트의 양이 적게 형성되는 사실에 기인하며, 변형에 따른 α 마르텐사이트 변태는 교류자화율과 금속입자 시험으로 알 수 있다.

Abstract Texture development and martensitic phase transformation, on rolling, are compared in two Hadfield's steels, one having low carbon content(0.65wt% C), the other high carbon content(1.35wt%). In spite of small difference in stacking fault energy(about 2 mJm^{-2}) between two Hadfield's steels, the differences in texture development are observed. In low carbon steel, the textures developed are similar to those of low stacking fault energy metals in low strain range. However, the abnormal textures such as {111}<uvw>, {110}<001> are strongly developed at high strain, which are due to the disturbance of α martensite in the development of textures formed at the packets of shear bands or at the grain boundaries. In contrast to low carbon Hadfield's steel(LCHS), the texture development of high carbon Hadfield's steel(HCHS) is similar to those of low stacking fault energy metals in the whole strain range. This may be due to the fact that the amount of deformation induced martensite was small, as observed by A.C. magnetic susceptibility and iron particle tests.

INTRODUCTION

The Hadfield's steels[1], which contains 10 to 14% Mn and 1 to 1.4% C, are used widely for many applications because of its outstanding resistance to abrasion are high work hardening rate. However, the influence of carbon in the development of deformation texture and phase transformation in Hadfield's steels(HS) has not been studied in detail.

Development of textures in face centred cubic(FCC) metals has been studied by many authors on a variety of systems; copper and brass[2), 3~5)], stainless steel[6, 7)], aluminium[8~10)], and Hadfield' steels[11)] and it is shown that the texture development is determined primarily by the stacking fault energy(SFE)[12)].

In low SFE metals such as 70-30 brass[3)] and stainless steels[6)], {110}<112>, {123}<634> are developed at low strain range and gradually become strong at medium strain range. But {123}<634> texture is destroyed and strong

{111}<110>, {110}<112> are developed at high strain. In contrast to low SFE metals, the {123}<634>, {110}<211> and {112}<111> are developed in low strain range and gradually become strong at high strain range in high SFE metals such as aluminium and pure copper[8), 13)].

Even though it has been reported that the alloy element carbon has an influence tending to increase the SFE of HS[14)] and stainless steel [15)], the SFE difference between two Hadfield's steels which is used in this study, is measured quite small($2mJm^{-2}$) (Low carbon HS, 0.65% C : High carbon HS, 1.35% C)[16)].

In the present study, the development of textures accompanying rolling in two HS is examined as a function of strain using pole figures, A.C. magnetic susceptibility and iron particle tests in order to find factors which influence the texture development.

EXPERIMENTAL PROCEDURE

Slabs of low carbon HS(LCHS, 0.65 %C) and high carbon HS(HCHS, 1.35 %C) were prepared by casting and hot rolling(Table 1). A specimen was cut from a hot rolled slab into a suitable size for cold rolling and the cut pieces were heat treated to make a homogenised structure(Table 2). The cold rolling was performed at strains of 20%, 40%, 60%, 80% and 90%. At each stage, a 5mm long specimen was cut for pole figure acquisition, A.C. magnetic susceptibility measurement and the iron particle test, while the thickness of the sample was measured to calculate the percentage reduction. These samples were then stored below 0℃ to minimise recovery effects prior to examination.

Table 1. Chemical compositions of the Hadfield's steels used in this study

Wt. %

	C	Mn	Si	S	P	Ni	Cr	Mo
LCHS	0.65	12.1	0.27	0.007	0.005	0.01	0.12	0.01
HCHS	1.35	13	0.06	0.016	0.007	0.01	0.11	0.03

Table 2. Heat treatment of the Hadfield's steels

	C(%)	Temp.	Time	Quench. Media
LCHS	0.65	1100℃	88hrs	water
HCHS	1.35	1100℃	72hrs	water

For texture measurement, the deformed specimen was cut to dimensions of 20×20mm and the centre was polished mechanically and chemically(10% oxalic acid) because it is necessary to eliminate surface texture on the rolling plane.

The polished specimen was mounted in a pole figure X-ray diffractometer connected to PDP/11 computer. The rolling direction was placed parallel to the direction of X-ray beam. A Co tube(wave length 1.79Å) was used because the absorption edge of Fe is 1.74 Å. (111) pole figures were determined by the Schulz back reflection techniques using Phillips PW 1010 X-ray diffraction unit fitted with PW 1078 texture goniometer. Intensity were measured every 7.5° along a spiral of 5° pitch and automatically recorded on a PDP/11 computer. The intensity contours were related to the intensity obtained from a sample which had a random texture.

Martensitic phase transformation occurs during cold rolling. In order to detect the α phase, which is ferromagnetic, the A. C. magnetic susceptibility of each specimen was measured. For comparison of the magnetic moments, specimen dimensions were kept constant to within 10% and the volume of each specimen was calculated by the mass of specimen divided by its density. The frequency was set at 83 Hz and the current at 300mA. In order to identify the magnetic phase in transverse direction(TD) section of the specimen, carbonyl iron powder (ferromagnetic) was spread with a fine brush on TD sections of the specimens and the results was photographed.

RESULTS AND DISCUSSION

1. Texture development

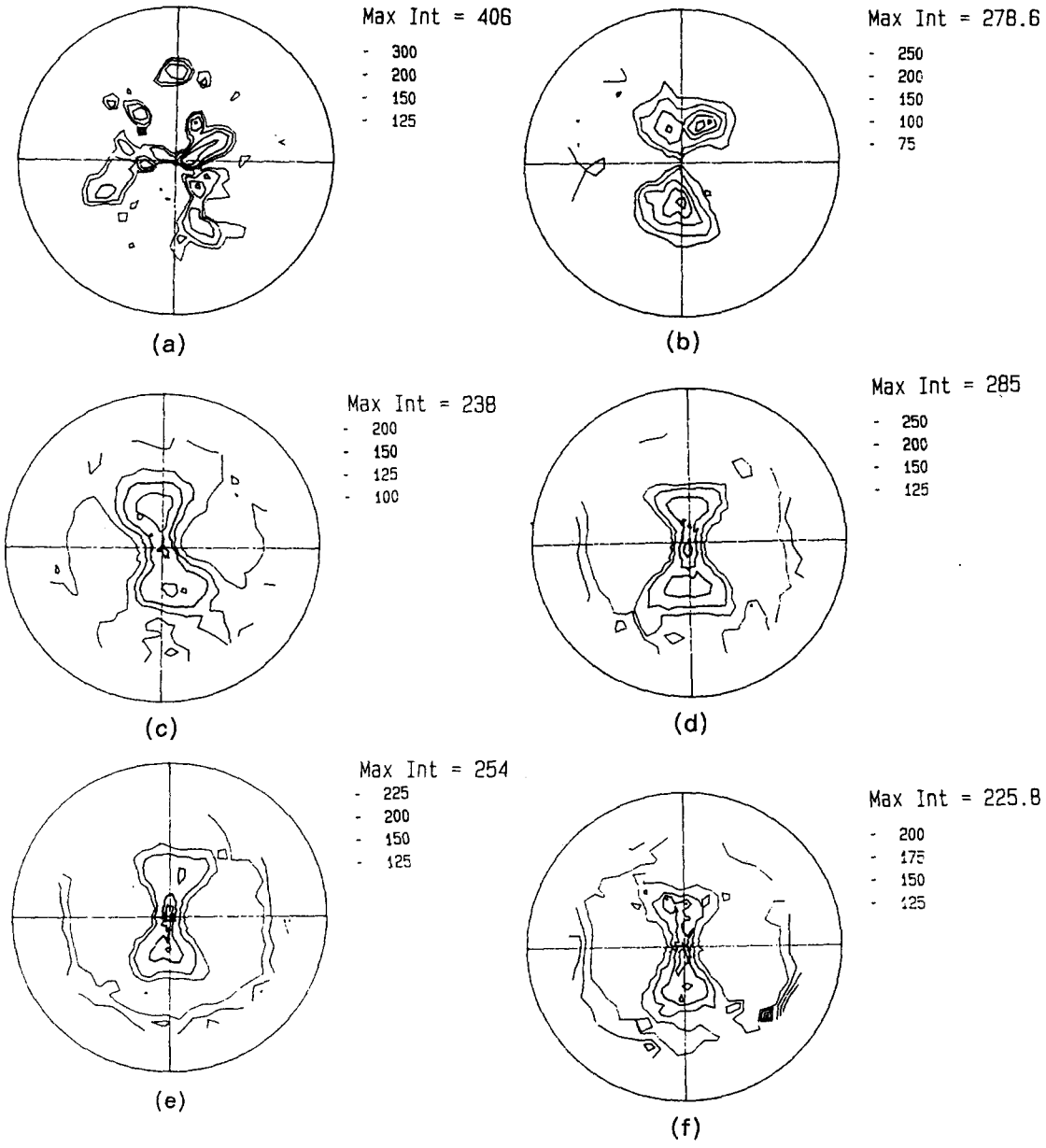

Fig. 1. (111) pole figures of rolled LCHS.
(a) ϵ=22% deformation (b) ϵ=39% deformation (c) ϵ=60% deformation (d) ϵ=80% deformation
(e) ϵ=87% deformation (f) ϵ=92% deformation

(1) Low carbon Hadfield's steel

The development of texture in LCHS with increasing strain is shown in Fig. 1 and Table 3. It is found that textures are different from those of low SFE FCC alloys(SFE<20 mJm^{-2}) such as 70-30 brass[3], 18-8 stainless steel[6]. In contrast to the transition textures in 70-30 brass, the transition texture {110}<001> which occurs at 39% deformation(Fig. 1(b)), gradually changes to {110}<112> texture until 80% defromation (Fig. 1(d)) with yet improved alignment at 92% deformation. Even though the strong {110}<211> texture dominates in 70-30 brass at high deformation(Fig.

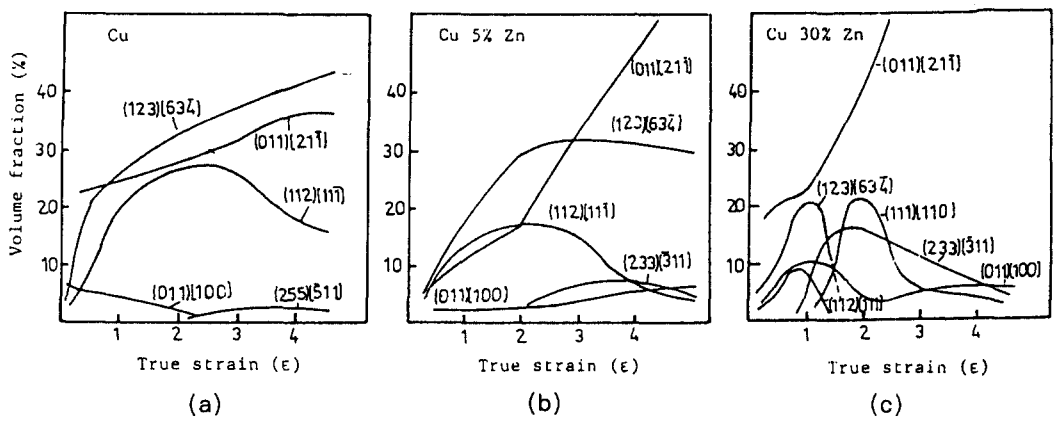

Fig. 2. Volume fraction of various texture components with deformation in pure Cu and two brass(Ref. 5)

Table 3. Major Texture components of LCHS, 70-30 brass and 18/8 stainless steel with strains

1. LCHS					
22%	40%	60%	80%	87%	92%
{110}	{110}<001>	{111}<uvw>	{111}<uvw>	{111}<uvw>	{111}<uvw>
{001}	{110}<112>	{110}<001>	{110}<112>	{110}<112>	{110}<001>
{123}	{123}<634>	{110}<112>	{110}<001>	{110}<001>	
{111}					
{112}					
2. 70-30 brass*					
	{011}<211>	{011}<211>	{011}<211>	{011}<211>	{011}<211>
	{123}<634>	{123}<634>	{111}<110>	{111}<110>	{111}<110>
	{011}<100>	{011}<100>	{233}<311>	{233}<311>	{233}<311>
	{112}<111>	{112}<111>	{011}<100>		
3. 18/8 stainless steel					
	{110}<112>	{110}<001>*2		{110}<112>	

*J. Hirsch and K. Lücke, 1988 [5];

*2 65% deformation

2), the strong texture of LCHS above 80% deformation is {111}<uvw> (Fig. 1 (c)-(f)) and this {111}<uvw> texture approaches {111}<110> at 92% deformation (Fig. 1 (f)). However, the {110}<112> texture component gradually changes to {110}<001> at 92% deformation. Moreover, this texture development in LCHS is not similar to that of 18-8 stainless steel which shows {110}<112> texture during deformation(Table 3). This fact suggests that the transition texture in LCHS is different from that of low SFE alloys.

In order to examine the {111} transition texture in LCHS, the relative intensities of (111) and (220) textures are calculated from the X-ray intensity of the specimen(Table 4). The {110} texture increases rapidly at about 40% deformation and decreases at about 60% deformation, but the {111} texture gradually increases and reaches a similar intensity to the

Table 4. Relative intensity of (111)/(200), (220)/(200) and (111)/(220) difraction X-ray in deformed LCHS

	0%	22%	39%	60%	80%	90%
(111)/(200) P	1	0.7	1.5	1.8	1.3	1.1
(111)/(200) I	1	0.7	1.2	1.5	1.1	1
(220)/(200) P	1	1.2	3.8	1.4	1.2	1.3
(220)/(200) I	1	1.3	3.1	1.5	1.6	2
(111)/(220) P	1	0.6	0.4	1.2	1.2	0.9
(111)/(220) I	1	0.6	0.4	1.0	0.7	0.5

*P and I stand for peak and integral intensity

{110} texture. This corresponds very well with the results of pole figure diagrams. This implies that in deformed LCHS the {111} transition textures are broadly distributed and become strongly textured at high deformation. In other words, the {111} transition texture exists stably from low strain to high strain, unlike 70-30 brass, where this texture only occurs at high strain. However, the {110} texture has a maximum intensity at 40% deformation. Thus, the texture development in LCHS is mainly composed of two components: {110} and {111}. The {110}<001> transition texture has a maximum intensity at about 40 % deformation and its intensity decreases at high deformation to an intensity similar to that of {111}<uvw> texture. But the {110}<001 > texture remains as a strong texture component, along with {111}<uvw>, at 92% deformation. However, the intensity of {110}<112 > texture gradually increases up to 80% deformation and decreases at 92% deformation. This implies that the texture development in LCHS is similar to that of 70-30 brass at low strain (up to 60% deformation), but is quite different from the low SFE alloys at high deformation(>60%).

(2) High carbon Hadfield's steel

The development of texture in HCHS with increasing strain is similar to that of 70-30 brass(Table 5, Fig 3). The intensity of {110}

Table 5. Major texture components of HCHS with strains

Def.	20%	40%	60%	80%	87%
texture	{001}	{110}<001>	{111}<uvw>	{110}<001>	{110}<112>
	{123}	{123}<634>	{110}<001>	{111}<110>	{111}<110>
	{112}	{110}<112>*	{110}<112>	{110}<112>	
	{111}		{123}<634>		
	{113}				

*minor component

<001> and {123}<634> transition textures is strong at 40% deformation and decreases with increasing deformation. But the transition texture {111}<uvw> occurs at about 60% deformation and strongly exists until 87% deformation. When the results are compared with texture development of 70-30 brass, it is suggested that the SFE of HCHS is similar to that of 70-30 brass.

In order to examine the {111} and {110} transition textures in HCHS, the relative intensities of (111) and (220) X-ray diffraction is

Table 6. Relative intensity of (111)/(200), (220)/(200) and (111)/(220) diffraction X-ray in deformed HCHS

Deformation	0%	20%	40%	59%	80%	87%
(111)/(200) P	1	1.5	2.3	4.9	5.7	2.2
(111)/(200) I	1	1.3	2.1	4.0	4.5	2.4
(220)/(200) P	1	1	15.5	5.0	11	5.0
(220)/(200) I	1	1	15.2	4.3	10.2	7.1
(111)/(220) P	1	1.2	0.1	0.8	0.4	0.5
(111)/(220) I	1	1.4	0.1	1.0	0.5	0.4

*P and I stand for peak and integral intensity

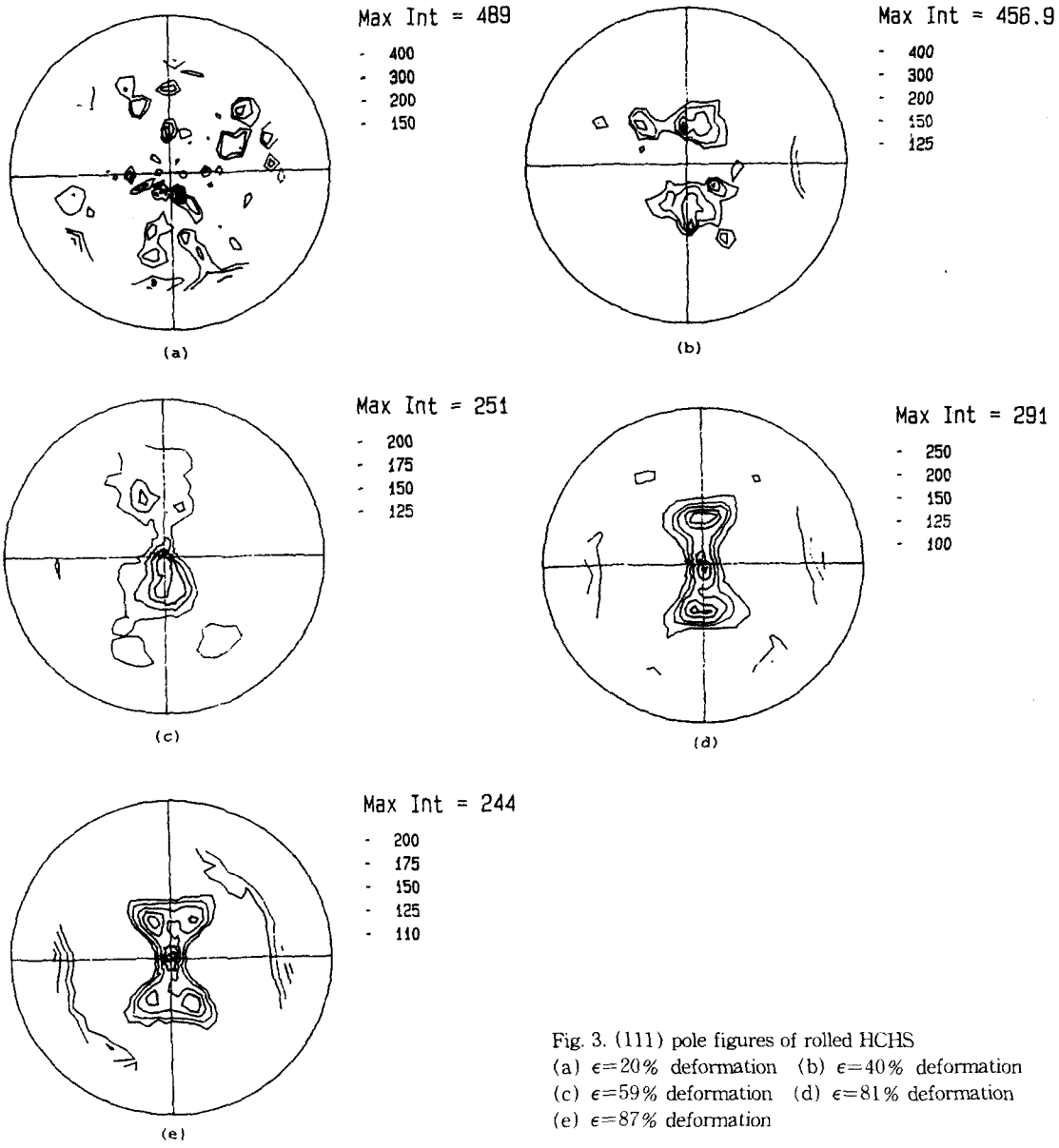

Fig. 3. (111) pole figures of rolled HCHS
(a) ϵ=20% deformation (b) ϵ=40% deformation
(c) ϵ=59% deformation (d) ϵ=81% deformation
(e) ϵ=87% deformation

revised in Table 6. The (220)/(200) X-ray intensity increases very rapidly at 40% deformation and decreases at 60% deformation. However, the (111)/(200) X-ray intensity ratio gradually increases up to 80% deformation and decreases at 87% deformation. As discussed in ref. (1), this maximum {220} X-ray intensity at 40% deformation is due to the {110}<001> transition texture and this transition texture gradually changes to {110}<112> texture with strains (Fig 3 (c), (d), (e)). Even though the {111} X-ray intensity gradually increases up to 80% deformation, the {111} <uvw> transition texture occurs at 60% deformation in (111) Pole figures (Fig. 3(c)). These facts correspond well with the texture development of 70-30 brass.

2. Martensitic phase transformation

(1) Low carbon Hadfield's steel

The measured values of A.C. magnetic

susceptibility are illustrated in Fig. 4. The magnetic susceptibility, which are supposed to increase due to the BCC phase transformation, (α martensitic transformation, ferromagnetic) rapidly increases at about 40% deformation. This appears to be related to the formation of shear bands because the shear bands begins to appear at about 40% deformation[16]. In order to identify the magnetic phase, occurring at 23 %, 38%, 54% and 69% deformed LCHS, ferromagnetic carbonyl iron powder, was spread with a fine brush on TD sections of the specimens. The results are shown in Fig 5. At 23% or 38% deformation, the iron particles are distributed randomly over TD section, which implies that the deformation twins or stacking faults[16] which formed within this deformation range have nothing to do with the magnetic phase transformation of LCHS. However, in 54% and 69% deformed LCHS, the iron particles are distributed on darkly etched areas such as shear bands. This facts correspond with the results of A.C. magnetic susceptibility measurements. It is implied that the favourable sites for martensitic phase transformation are either at the boundaries of the packets of shear bands or at the grain boundaries[16].

As is shown in Fig. 5 (e), the iron particles grow upright at the boundaries of packets of

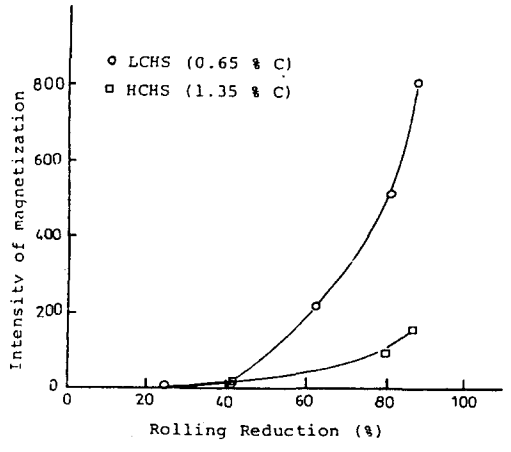

Fig. 4. Relative intensity of magnetization of LCHS with various rolling reductions at room temperature.

shear bands or at the grain boundaries. This suggests that the magnetic phase has a preferred magnetized texture which induced the ferromagnetic phase. The fact could be explained using the direction of easy magnetization in FCC metals and the texture development in LCHS. The direction of easy magnetization of FCC Nickel is the body diagnals $<111>$[17], and the texture developed at about 90 % deformation in LCHS is $\{111\}<uvw>$ and $\{110\}<001>$. According to the Bain correspondence, the orientation relationship between γ phase (FCC) and α phase (BCC) in martensitic phase transformation of stainless steel is $(111)_\gamma//(011)_\alpha$, $[\bar{1}01]_\gamma//[\bar{1}\,\bar{1}1]_\alpha$. Thus, we can draw the schematic martensitic phase transformation as in Fig. 6. There are two possible configurations of unit cells in 92 % deformed LCHS: (a) $\{110\}<001>$ rolling texture and (b) $\{111\}<uvw>$ rolling texture. Thus, on a TD section of deformed LCHS, the orientation of the γ phase could be $(1\bar{1}0)[\bar{1}10]$ or $(\bar{1}10)$, $[\bar{1}10]$. This orientation is the most favourable for the α martensitic phase transformation, i.e. the possible $\{110\}<111>$ α phase could occur in the shadow region in Fig. 6. In other words, the preferred magnetization along the $<111>$ direction of α (BCC) phase occurred perpendicular to TD section of deformed LCHS. This preferred magnetizaiton grows parallel or 35° to rolling direction (RD) because $(111)_\gamma$ plane aligned to such angles to rolling direction in the unit cells as in Fig. 6. This corresponds with the upright stature and parallel or 35° extension of iron particles to RD on TD section of LCHS.

Thus, the α martensitic phase transformation occurs at the boundaries of packets of shear bands or at the grain boundaries after about 40% deformation. This could be related with the formation of shear bands which would supply the favourite sites for α martensite formation. This α martensite formation is thought to disturb the development of texture in LCHS because the Bain correspondence, the orienta

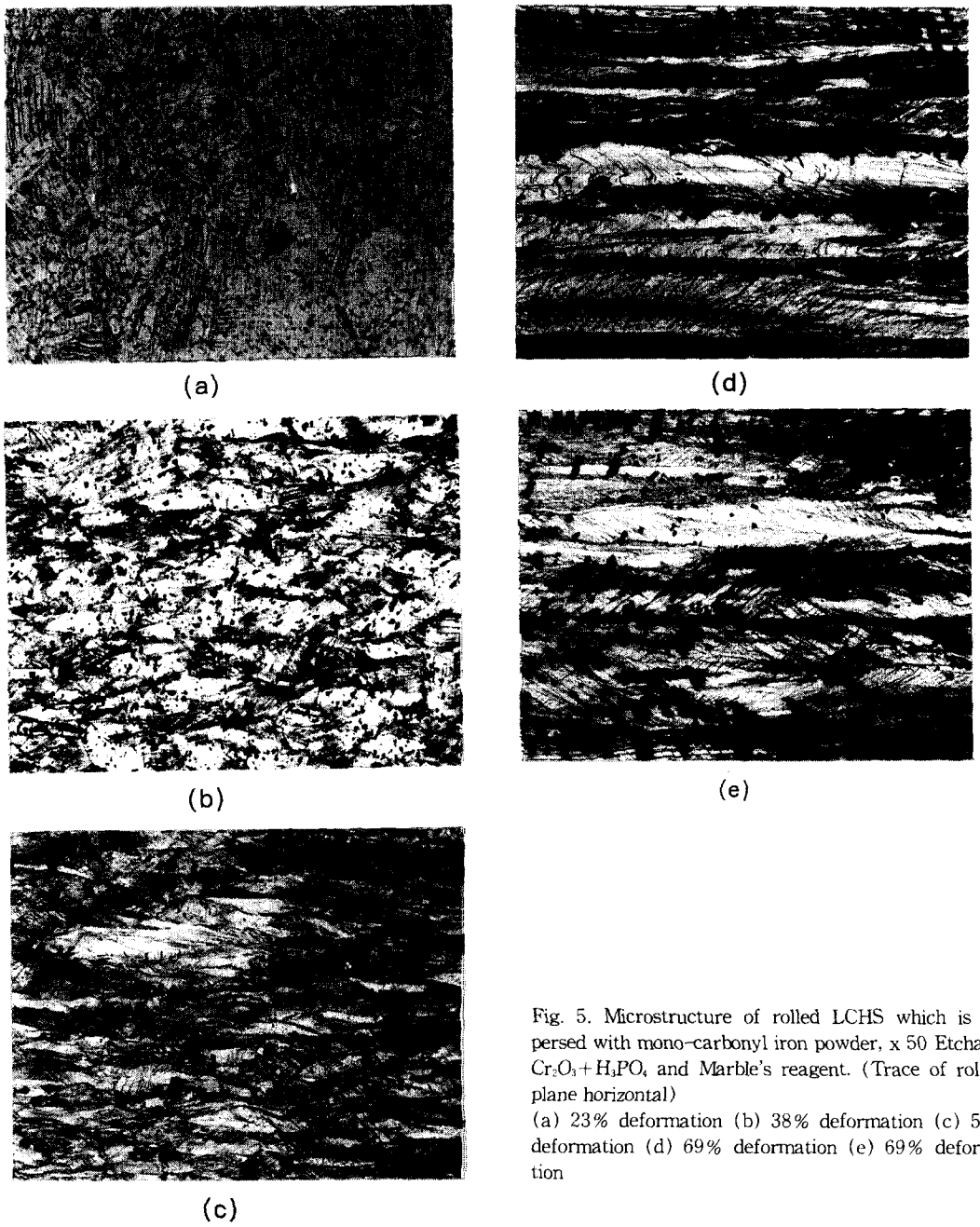

Fig. 5. Microstructure of rolled LCHS which is dispersed with mono-carbonyl iron powder, x 50 Etchant: $Cr_2O_3+H_3PO_4$ and Marble's reagent. (Trace of rolling plane horizontal)
(a) 23% deformation (b) 38% deformation (c) 54% deformation (d) 69% deformation (e) 69% deformation

tion relationship $(111)_\gamma//(110)_\alpha$, $[\bar{1}01]_\gamma//[\bar{1}\,\bar{1}1]_\alpha$ between α and γ phase, is also valid in deformed LCHS, as confirmed by texture development and the iron particle test.

(2) High carbon Hadfield's steels

In contrast to LCHS, the A.C. magnetic suscepibility value is relatively low at high deformation as shown in Fig. 4. This implies that the amount of α phase transformation is small compared to that of LCHS.

The results of the iron particle test is shown in Fig. 7. At 21%, 42% and 61% deformation, the iron powder particle distributed homogeneously, but at 81% deformation the iron particles are attracted to the boundaries of packets of shear bands or grain boundaries (Fig 7(d)).

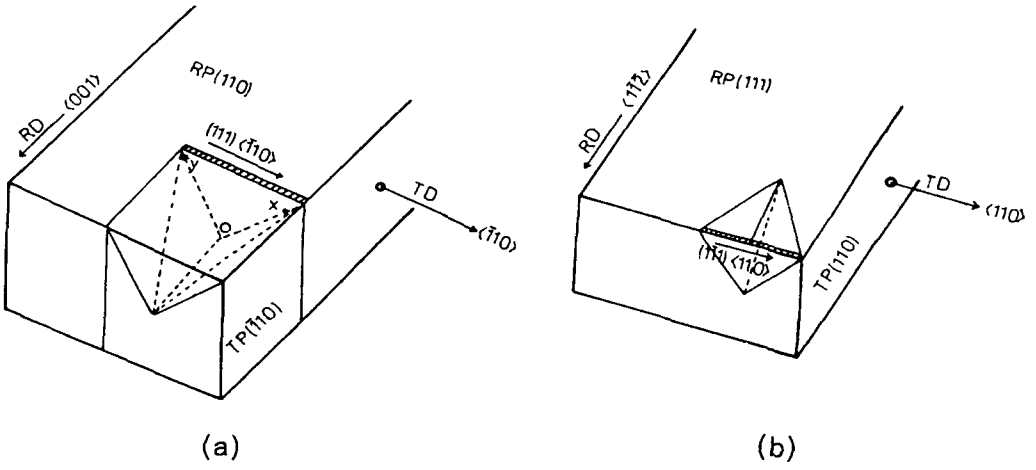

Fig. 6. Schematic drawing of α martensitic phase transformation using the results of rolling texture and the Bain orientation relationship between γ (FCC) and α (BCC) phase. The shadow is the most possible regions that the α martensitic phases can be observed.
(a) (110)<001> texture
(b) (111) <uvw>texture
RD: Rolling direction,
TD: Transverse direction
RP: Rolling plane
TP: Transverse plane

This implies that the favourite sites for α martensitic phase transformation are grain boundaries or at the boundaries of packets of shear bands in deformed HCHS, which is similar to LCHS.

In contrast to LCHS, the iron particles are distributed nearly parallel to RD on TD section at 81% deformation (Fig. 7(d)). This implies that <111> easy magnetization of α phase (BCC) would be aligned parallel to TD section. This fact can be explained by the texture development in HCHS. As described in texture of HCHS, the major texture is {110}<112> and {111}<110> at about 87% deformed HCHS. This texture and the Bain orientation relationship between γ and α phase would produce the (111)[111] and $(\bar{1}\,\bar{1}2)[\bar{1}\,\bar{1}2]$ normal to the TD section (Fig. 8), which would most likely produce strong magnetization (<111>BCC) parallel to the TD section or at 35° to RD because $(111)_\gamma$ aligned to such angles to RD in the unit cells as in Fig. 8. In other words, the direction of magnetization would be parallel or in some angles to RD section of specimen. This fact corresponds with the results of the iron particle test (Fig 7(d)):i. e. in some area, the iron particles are distributed nearly parallel to RD (marked A in Fig 7 (d)) but in other area the iron particles are aligned about 20° to RD (arrow marked in Fig. 7(d)).

Thus, it is thought that the small amount of α martensite formation in HCHS does not disturb the development of texture.

CONCLUSIONS

(1) The texture development of LCHS is similar to that of low stacking fault metals at low strain range. However, the abnormal {111}<uvw> and {110}<001> texture is strong at high strain (92% deformation) and the intensity of A.C. mignetization is high at this strain. This implies that the formation of α martensite at the packets of shear bands or at the grain boundaries, disturbs the texture development of LCHS at strain>60%.

(2) In contrast to LCHS, the texture devel-

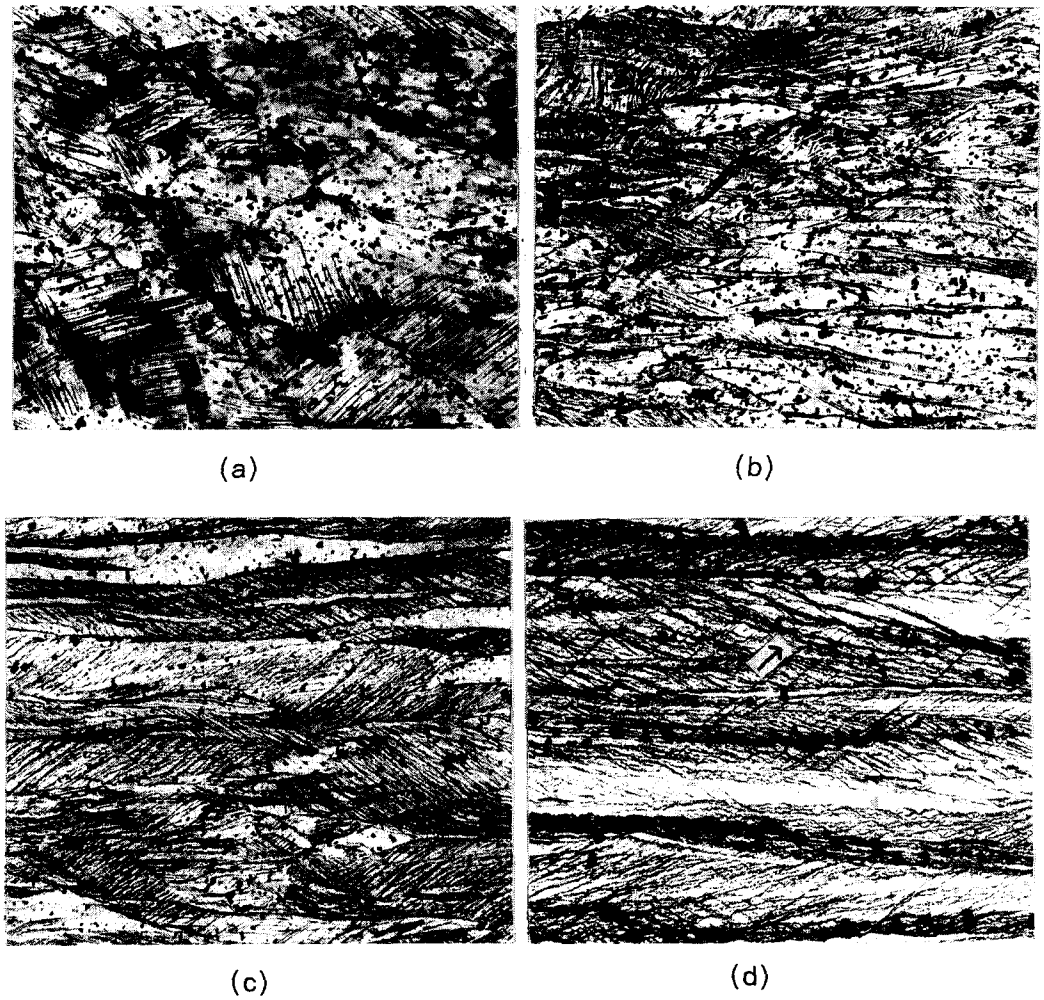

Fig. 7. Microstructures of rolled HCHS which is dispersed with mono-carbonyl iron powder, Etchant: $Cr_2O_3+H_3PO_4$ and Marble's reagent.
(a) 21% deformation (b) 42% deformation (c) 61% deformation (d) 81% deformation
(Trace of rolling Plane horizontal)

opment of HCHS is similar to that of low SFE metals in the full range of strain, which is well corresponds with low intensity of A.C. magnetic susceptibility value. In other words, the deformation induced α phase transformation at the packets of shear bands or at the grain boundaries does not disturb the development of texture because the amount of α phase transformation is small.

Acknowlegement

This study was financilally supported by a central reseach fund in 1995 from PaiChai university.

REFERENCES

1. American Society for Testing and Materials, Standard Specification for Steel Castings, Austenitic Manganese: A 128/A 128M-86, 01.02, 84, Annual Book of A.S.T.M. Standards.
2. A.S. Malin and M. Hatherly, Met. Sci., 13, 463(1979).
3. W.B. Hutchison, B.J. Duggan and M.

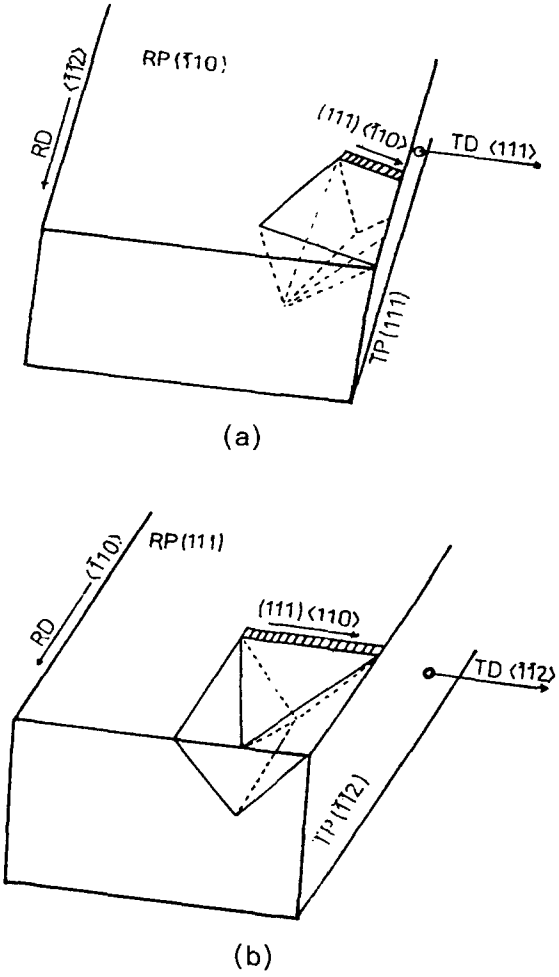

Fig. 8. Schematic drawing of α martensitic phase transformation using the results of rolling texture and the Bain orientation relationship between γ (FCC) and α (BCC) phase. The shadow is the most possible regions that the α martensitic phases can be observed.
(a) (110)<112> texture,
(b) (111)<110> texture
RD: Rolling direction
TD: Transverse direction
RP: Rolling plane
TP: Transverse plane

Hatherly, Metals Technology, 398(1979).
4. P.T. Wakefield and M. Hatherly, Met. Sci., 109(1981).
5. J. Hirsch, K. Lüche and M. Hatherly, Acta Metall., 36(11), 2905(1988).
6. Y. Sato, T. Sakai, K. Tajeda and K. Kato, Trans ISIJ, 25, B-275(1985).
7. J.N. Reissner, 'The influence of Texture Anisotropy on the Deformation Forming Limits of Austenitic Stainless Steel Sheet' in Gottstein, G. and Lücke, K. (Eds), Op. Cit., 2, 475, (1978).
8. K. Lücke and J. Hirsch, 'Rolling and Recrystallization Textures of Aluminium', private communication.
9. J. Hirsch, E. Nes and K. Lücke, Acta Metall., 35(2), 427(1986).
10 A.L. Dons and E.Nes, Mat. Sci. Techn., 2, 8 (1986).
11. P.H. Adler, G.B. Olson and W.S. Owen, Met. Trans.A, 17A, 1725(1986).
12. K. Lücke and K.H. Virnich, In fifth Conf. ' Textures of Materials', Aachen, Springer-Verlag, 1, 397(1987).
13. M.Y. Huh, J. Hirsch and K. Lücke, in 7th international conference on textures of materials, Ed. C.M. Brakman, P. Jongenburger, E.T. Mittemeijer, 601 (1984), Netherlands.
14. P.Yu. Volosevich, V.N. Gridnev and Yu.N. Petrov, Fiz. Metal. Metalloved., 40(3), 554 (1975).
15. R. Fawley, M.A. Quader and R.A. Dodd, Trans. TMS-AIME, 242, 771(1968).
16. T.N. Kim and A.J. Bourdillon: J. Mat. Sci. and Techn., 8, 1011-1021(1992).
17. R.M. Bozorth: 'Ferromagnetism', Van Norstrand, 1951.